PCCP

PAPER

Cite this: *Phys. Chem. Chem. Phys.*, 2018, **20**, 19398

Effects of intramolecular hydrogen bonding and sterically forced non-coplanarity on organic donor/acceptor two-photon-absorbing molecules

David J. Stewart, *[ab] Ramamurthi Kannan,[ac] Tod A. Grusenmeyer,[ab] Jacob M. Artz,[ad] Stephanie L. Long,[ad] Zhenning Yu,[ac] Thomas M. Cooper,[a] Joy E. Haley[a] and Loon-Seng Tan*[a]

Two photon absorption (2PA) is of great interest across many disciplines and there has been a large effort to increase the two-photon cross section (σ_2) *via* synthetic modification, especially by enhancing intramolecular charge-transfer (ICT). This work takes the previously studied (7-benzothiazol-2-yl-9,9-diethylfluoren-2-yl)diphenylamine (**AF240**), an asymmetric D–π–A chromophore, and intentionally appends a functional group (–OH, **AF240-OH** or $-OCH_3$, **AF240-OMe**) to the 6-position of the fluorenyl π-bridge of the new chromophores. Electrochemical results in both dichloromethane and acetonitrile support stabilization of the highest occupied molecular orbital in the derivatives due to inductive electron donating effects of the hydroxy and methoxy groups. The lowest unoccupied molecular orbital is stabilized *via* intramolecular hydrogen bonding to the benzothiazole moiety in the case of **AF240-OH**. As previously observed for **AF240**, the steady-state emission spectra show significant solvatochromism as they broaden and red shift with increasing solvent polarity. The fluorescence lifetimes and quantum yields show that the non-radiative rate constant is increased for **AF240-OH** in all solvents, especially in nonpolar media. The results suggest there is forced intramolecular hydrogen bonding to the benzothiazole in nonpolar solvents because the solvent poorly solubilizes the hydroxy group. This increases the non-radiative decay rate constant (k_{nr}) *via* additional vibrational decay pathways. While not as dramatic, the increase in k_{nr} in polar solvents supports some deactivation *via* hydrogen bonding to the solvent. Steric effects are also observed in the methoxy derivative, which inhibits planarization of the benzothiazole with the fluorene, increasing the energy of the excited state. Ultrafast transient absorption spectroscopy in tetrahydrofuran solution supports stabilization of the excited state in a few ps as solvent and structural reorganizations occur. In the case of **AF240-OH**, no evidence of proton transfer is observed. The decrease in emission energies in the case of **AF240-OH** support increased ICT driven by higher degree of coplanarity and the quinoidal structure in the excited state. However, a moderate increase in the intrinsic 2PA cross-section is resulted. It is likely because of the two possible and competing solvent-stabilized ICT processes (PICT and TICT) in **AF240-OH**. Nevertheless, the strategic presence of a hydroxide group capable of intramolecular hydrogen bonding in **AF240-OH** provides a much broader 2PA sensitivity window than **AF240**.

Received 25th April 2018,
Accepted 7th July 2018

DOI: 10.1039/c8cp02647e

rsc.li/pccp

Introduction

Two-photon absorption (2PA) has wide-ranging applications such as microscopy,[1–3] microfabrication,[4,5] photodynamic therapy,[6] and nonlinear absorption.[7–9] It is well understood that an increase in the intramolecular charge-transfer (ICT) character can significantly enhance the 2PA cross section, σ_2.[10–15] A common strategy to accomplish this involves incorporating electron donor (D) and acceptor (A) groups within a molecule to induce dipole moment changes which lead to increased ICT.[16–19] One successful synthetic design is *via* a D–π–A motif with the π-bridge being a fluorenyl group.[20–26] For example **AF240**, which contains a fluorenyl core with a diphenylamino donor and benzothiazole acceptor, has a 2PA cross section of $50 \pm 8 \times 10^{-20}$ cm^4 GW^{-1}.[27] As shown previously,[28] **AF240** planarizes in the excited state about both the diphenylamino-fluorene and benzothiazole-fluorene bonds. However, by adding bulky substituents in

[a] *Air Force Research Laboratory, Materials and Manufacturing Directorate, Functional Materials Division, Wright-Patterson AFB, Ohio 45433-7750, USA. E-mail: david.stewart.32.ctr@us.af.mil, loon.tan@us.af.mil*
[b] *General Dynamics Information Technology, 5100 Springfield Pike, Dayton, Ohio 45431, USA*
[c] *UES, Inc., 4401 Dayton-Xenia Road, Dayton, Ohio 45432, USA*
[d] *Southwestern Ohio Council for Higher Education, Dayton, Ohio 45420, USA*

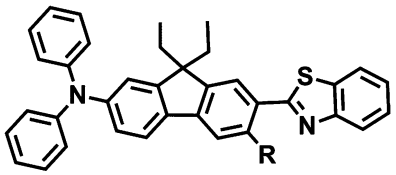

AF240-R

R = H, OH, OMe

Fig. 1 Structure of the molecules.

appropriate molecular locations and impeding the bond rotations necessary for planarization, the extent of ICT can be diminished, and transition dipole moment, greatly reduced.

In addition to sterics affecting the excited state, one could imagine both inter- and intramolecular hydrogen bonding playing a role. This has been shown in derivatives of 2-(2′-hydroxyphenyl)-benzothiazole (HBT), where excited-state intramolecular proton transfer (ESIPT) is typically observed.[29–33] However, in 2-(2′-aminophenyl)benzothiazole derivatives, ESIPT can be kinetically controlled or completely eliminated by modifying the substituents on the amino group and in the 5-position of the phenyl ring.[34] Hydrogen atoms or methyl groups as substituents prevented ESIPT, while adding electron-withdrawing groups not only allowed for ESIPT but also increased the rate with increasing withdrawing strength. In the absence of ESIPT, hydrogen bonding can still impact excited states by lowering their energies or decreasing their lifetimes *via* increased vibrational decay pathways.[35–37]

It is noteworthy that the fluorenyl analog of HBT, *i.e.* the *ortho*-OH is on fluorene instead of phenyl unit, has not been synthesized despite the fact that fluorenyl offers longer conjugation length than phenyl and greater planarity than biphenyl.[38] In this report, two new **AF240** derivatives (Fig. 1) are synthesized and their photophysical properties examined. The new derivatives contain a hydroxy (**AF240-OH**) or methoxy (**AF240-OMe**) group in the 6-position of the fluorenyl π-bridge. The three molecules allow for the effects of electronics, sterics, and hydrogen bonding to be observed and compared.

Experimental

Cyclic voltammetry

Voltammograms were obtained using a CH Instruments CH620E Electrochemical Analyzer. The working electrode was a glassy-carbon electrode (electrode area = 0.707 cm^2), the counter electrode was a Pt wire, and the reference electrode was an aqueous Ag/AgCl (4 M KCl) electrode. Data were collected in dichloromethane and acetonitrile solution containing 0.1 M $TBAPF_6$. The dichloromethane and acetonitrile were dried over activated, 3 Å molecular sieves for 24 hours prior to solution preparation.[39] The samples were bubble deaerated with argon for 10 minutes prior to data collection.

Instrumentation

NMR spectra were obtained using a Bruker Avance 400 MHz spectrometer, and chemical shifts were referenced to the solvent residual peak.

Ground-state UV/vis absorption spectra were measured on a Cary 5000 spectrophotometer. Fluorescence spectra were obtained using an Edinburgh Instruments FLS980 spectrometer using excitation at the absorption peak maxima. Fluorescence quantum yields were obtained using the FLS980 equipped with an integrating sphere. Time-correlated single-photon counting (Edinburgh Instruments OB920 spectrometer) was utilized to determine excited state lifetimes. The samples were excited using a 70 ps laser diode at 375 nm. Fluorescence was detected on a cooled microchannel plate PMT. Data were analyzed using a reconvolution software package provided by Edinburgh Instruments. All experiments were performed at room temperature.

Ultrafast transient absorption measurements were performed using a modified version of the femtosecond pump–probe UV-VIS spectrometer described elsewhere.[40] Briefly, 4 mJ, 45 fs pulses at 785 nm at 1 kHz repetition rate were obtained from a cryogenically-cooled, Ti:Sapphire regenerative amplifier (KM Labs Wyvern 1000-10). Approximately 5% (0.2 mJ) was reflected into the experiment, which was split into pump and probe (90 and 10%, respectively) by a beam splitter. The pump beam was directed into a frequency doubler (CSK Super Tripler) and then was focused into the sample. The probe beam was delayed in a computer-controlled optical delay (Newport MM4000 250 mm linear positioning stage) and then focused into a sapphire plate to generate white light continuum. The white light was then overlapped with the pump beam in a 2 mm quartz cuvette and then coupled into a CCD detector (Ocean Optics S2000 UV-VIS). Data acquisition was controlled by software developed by Ultrafast Systems LLC.

Femtosecond two-photon induced fluorescence (2PIF) spectral measurements were conducted at Montana State University under a service agreement, using the experimental set-up as described previously[41] with 4,4′-bis-*N*,*N*′-(diphenylamino)stilbene (BDPAS) in CH_2Cl_2 as reference standard for **AF240** and **AF240-OH** and fluorescein in water at pH 11[42] for **AF240-OMe**. The resulting intrinsic 2PA cross-sections are expressed in GM unit (1 GM = 10^{-50} cm^4 s $photon^{-1}$ $molecule^{-1}$) and have ±15% measurement uncertainty.

Materials and methods

High purity solvents were obtained from commercial vendors and used as received. All reagents, palladium complexes and phosphine-based ligands used in the syntheses of the chromophores were obtained from Aldrich. The synthesis of **AF240** has been previously reported.[21]

2-(7-Bromo-9,9-diethyl-3-acetoxy-2-fluorenyl)benzothiazole (2). A mixture of 2-(7-bromo-9,9-diethyl-2-fluorenyl)benzothiazole (**1**, 10.85 g, 25 mmol), iodobenzene-1,1-diacetate (8.74 g, 27.13 mmol), acetic anhydride (10.0 mL, 105.8 mmol), palladium(II) acetate (280.64 mg, 1.25 mmol) and acetic acid (65 mL) was held at 114 °C for 8 hours. After cooling, it was

diluted with toluene, and the solution was washed with water, dried and concentrated under vacuum. The residue was dissolved in toluene, and the solution was washed with water, dried and concentrated. The dark oil that was left behind was chromatographed over silica gel and the column was eluted with 1 : 1 toluene–heptane and 3 : 1 toluene–heptane. Residue from earlier fractions was suspended in ethanol, and the bromofluorenylbenzothiazole starting material, 2.16 g, m.p. 117–119 °C was collected. Later fractions gave the acetoxy product after crystallization from a mixture of heptane and toluene, 5.48 g (45% yield, 56% adjusted for starting material recovery), m.p. 150.5–151.5 °C. Mass spec: *m*/*z* 491, 493. Anal. calc. for $C_{26}H_{22}NO_2SBr$: C, 63.40%; H, 4.50%; N, 2.84%; S, 6.51%; Br, 16.23%. Found: C, 63.42%; H, 4.50%; N, 2.87%; S, 6.52%; Br, 16.54%. ^{1}H NMR ($CDCl_3$), δ ppm: 0.37 (t, 6H, 7.28 Hz), 2.09 (m, 4H), 2.53 (s, 3H), 7.40 (m, 1H), 7.51 (m, 5H), 7.92 (d, 1H, 8.0 Hz), 8.10 (d, 1H, 8.0 Hz) and 8.4 (s, 1H). ^{13}C NMR, δ ppm: 8.58, 21.69, 29.69, 32.63, 56.75 (5 sp^3C), 114.82, 121.28, 121.92, 122.63, 123.22, 124.04, 124.80, 125.27, 126.34, 126.53, 130.41, 135.44, 138.92, 143.80, 147.31, 148.19, 152.84, 153.34, 162.80, and 169.04 (20 sp^2C).

2-(7-Bromo-9,9-diethyl-3-hydroxy-2-fluorenyl)benzothiazole (3). A mixture of **2** (4.15 g, 8.43 mmol), potassium carbonate (0.55 g, 3.98 mmol), tetrahydrofuran (25 mL) and methanol (9.0 mL) was stirred at room temperature for 16 hours, solvents were evaporated, and the residue was suspended in water. The solid crude product was filtered and then recrystallized from a mixture of heptane and toluene, 3.51 g (92% yield), m.p. 177–178 °C. Mass spec: *m*/*z* 449, 451. Anal. calc. for $C_{24}H_{20}NSOBr$: C, 64.00%; H, 4.48%; N, 3.11%; S, 7.12%; Br, 17.72%. Found: C, 64.00%; H, 4.50%; N, 3.12%; S, 7.12%; Br, 17.81%. ^{1}H NMR ($CDCl_3$), δ ppm: 0.40 (t, 6H, 12.6 Hz), 2.02 (m, 4H), 7.43 (m, 7H), 7.90 (d, 1H, 7.88 Hz), and 7.98 (d, 1H, 8.12 Hz). 13C NMR, δ ppm: 8.54, 32.91, 56.03 (3 sp^3C), 106.67, 115.89, 121.43, 121.93, 122.05, 122.54, 125.45, 126.37, 126.74, 130.35, 132.48, 139.40, 140.43, 145.21, 151.95, 153.51, 158.09, and 169.69 (18 sp^2C).

One-pot procedure for 3. A mixture of **2** (9.5 g, 21.9 mmol), diacetoxy iodobenzene (7.67 g, 23.82 mmol), palladium(II) acetate (226.0 mg, 1.01 mmol) and acetic acid (75 mL) was kept at reflux (110–115 °C) for 8 hours, and concentrated. The residue was dissolved in toluene and washed with water. After drying and concentration, the residue was dissolved in tetrahydrofuran (100 mL) and methanol (50 mL), and the solution was stirred with potassium carbonate (4.6 g, 33.3 mmol) at room temperature for 2 hours. The residue left after removal of solvents was dissolved in toluene and the solution was washed with water, dried and concentrated. The residue (14.96 g) was chromatographed over silica gel. Toluene–heptane 2 : 3, eluted the product, 4.85 g (49% yield), m.p. 175–177 °C. Starting benzothiazole, 1.48 g (15%), m.p. 117–120 °C, was recovered from 1 : 1 toluene–heptane eluates.

2-(7-Bromo-9,9-diethyl-3-methoxy-2-fluorenyl)benzothiazole (4). To a mixture of **3** (2.5 g, 5.55 mmol), potassium carbonate (1.47 g, 10.6 mmol) and *N*,*N*-dimethyl acetamide (10 mL), cooled in an ice bath, dimethyl sulfate (1.0 mL, 10.6 mmol) was added, and after 3 hours, the mixture was poured into water. The separated solid (2.63 g) was dissolved in 1 : 1 toluene–heptane, the solution was passed through a column of silica gel and the eluate collected was concentrated on a rotavap. The resulting solid residue was recrystallized from a mixture of heptane and toluene, 2.27 g (88% yield), m.p. 175–177 °C. Mass spec: *m*/*z* 463, 465. Anal. calc. for $C_{25}H_{22}BrNOS$: C, 64.66%; H, 4.77%; N, 3.02%; S, 6.90%; Br, 17.20%. Found: C, 64.66%; H, 4.77%; N, 3.04%; S, 6.90%; Br 17.65%. ^{1}H NMR ($CDCl_3$) δ ppm: 0.33 (t, 6H, 7.28 Hz), 2.09 (m, 4H), 4.1 (s, 3H), 7.30 (m, 2H), 7.50 (m, 3H), 7.59 (d, 1H, 8.52 Hz), 7.92 (d, 1H, 7.8 Hz), 8.09 (d, 1H, 8.08 Hz) and 8.49 (s, 1H). ^{13}C NMR, δ ppm: 8.53, 29.71, 32.69, 55.96, 56.50 (5 sp^3C), 102.92, 121.16, 121.36, 121.74, 122.25, 122.60, 123.48, 124.51, 125.90, 126.48, 130.18, 136.16, 139.67, 141.97, 143.99, 152.15, 153.74, 157.48 and 163.58 (19 sp^2C).

***N*,*N*-Diphenyl-7-(benzothiazol-2-yl)-9,9-diethyl-6-methoxyfluorene-2-amine (5; AF240-OMe).** A mixture of **4** (6.97 g, 15.0 mmol), diphenylamine (3.2 g, 18.75 mmol) and toluene (100 mL) was azeotroped dry and cooled. At 48 °C, bis-(dibenzylideneacetone)palladium(0) (132.0 mg, 0.23 mmol), 1,1′-bis-(diphenylphosphino)ferrocene (128.6 mg, 0.232 mmol) and sodium *t*-butoxide (2.48 g, 26.35 mmol) were added, and the mixture was heated to 94 °C, and held at that temperature for 5 hours. After cooling, it was diluted with toluene, and the solution was washed with water, dried and concentrated. The residue (10.24 g) was chromatographed over silica gel, and the column was eluted with 3 : 1 toluene–heptane to get the product that was recrystallized from a mixture of ethanol and toluene, 6.92 g (84% yield), m.p. 242–244 °C. Mass spec: *m*/*z* 552. Anal. calc. for $C_{37}H_{32}N_2OS$: C, 80.40; H, 5.82%; N, 5.07%; S, 5.80%. Found: C, 80.40%; H, 5.88%; N, 5.11%; S, 5.80%. ^{1}H NMR ($CDCl_3$), δ ppm: 0.38 (t, 6H, 7.2 Hz), 1.95 (m, 2H), 2.1 (m, 2H), 7.04 (m, 3H), 7.15 (m, 5H), 7.31 (m, 6H), 7.35 (t, 1H, 8.0 Hz), 7.48 (m, 1H), 7.92 (d, 1H, 8.0 Hz), 8.1 (d, 1H, 8.0 Hz), and 8.45 (s, 1H). ^{13}C NMR, δ ppm: 8.61, 29.94, 32.65, 55.94, 56.05 (5 sp^3C), 102.21, 118.81, 120.41, 120.77, 121.11, 122.46, 122.85, 123.11, 123.19, 124.20, 124.28, 125.78, 129.26, 135.39, 136.10, 142.31, 145.11, 147.87, 148.26, 152.23, 153.01, 157.57 and 163.93 (22 sp^2C).

***N*,*N*-Diphenyl-7-(benzothiazol-2-yl)-9,9-diethyl-6-hydroxyfluoren-2-amine (6; AF240-OH).** Under nitrogen, a mixture of **5** (5.53 g, 10.0 mmol), 2-aminothiophenol (2.2 mL, 20.56 mmol), potassium carbonate (0.48 g, 3.5 mmol) and 1-methylpyrrolidinone (35 mL) was kept at 200 °C for 3 hours, and cooled. The cooled mixture was poured into a mixture of ice and water containing acetic acid (15 mL), and the separated solid (6.02 g) collected. This was transferred to a column of silica gel, and the column was eluted with 3 : 1 toluene–heptane to get the product that was then recrystallized from a mixture of toluene and ethanol, 4.9 g (91%), m.p. 248–250 °C. Mass spec: *m*/*z* 538. Anal. calc. for $C_{36}H_{30}N_2OS$: C, 80.26%; H, 5.61%; N, 5.20%; S, 5.95%. Found: C, 80.06%; H, 5.62%; N, 5.18%; S, 6.03%. ^{1}H NMR ($CDCl_3$). δ ppm: 0.4 (t, 6H, 7.2 Hz), 1.9 (m, 4H), 7.05 (m, 4H), 7.15 (d, 4H, 8.0 Hz), 7.29 (m, 5H), 7.38 (t, 1H, 8.0 Hz), 7.5 (t, 1H, 8.0 Hz), 7.58 (d, 1H, 8.0 Hz), 7.9 (d, 1H, 8.0 Hz), and 7.95 (d, 1H, 8.0 Hz). ^{13}C NMR, δ ppm: 8.63, 32.86, 55.58 (3 sp^3C), 107.76, 114.67, 118.44, 121.38, 121.80, 121.86, 122.93, 123.12, 124.29, 125.18, 125.62, 129.27, 132.43, 135.04, 140.91, 146.35, 147.82, 148.52, 152.05, 152.82, 158.14, and 168.98 (22 sp^2C).

Results and discussion

Synthesis

The synthesis of **AF240** was accomplished in a four-step synthetic sequence, starting from commercially available 2,7-dibromofluorene, and has been reported.[21] The precursor to **AF240** was **1** which was used as the starting point in the synthetic route for both **AF240-OMe** (**5**) and **AF240-OH** (**6**) as depicted in Scheme 1. The synthetic objective is to functionalize an OR group *ortho* to the benzothiazolyl segment so that when OR is OH, intramolecular hydrogen bonding would occur as established in the crystal structure of HBT.[43] However, while the synthesis of HBT has been made easy by having *ortho*-hydroxylphenyl in the readily available salicylaldehyde, the synthesis of the fluorene analog presents a challenge as it requires a direct insertion of an oxygen atom in the 1 or 3 position (*i.e. ortho*-hydroxylation, see Scheme 1) and such synthetic tool was only developed very recently.[44] Following this method, the acetate intermediate (**2**) after the palladium-catalyzed acetoxylation of the bromo-fluorenylbenzothiazole compound (**1**) by iodobenzene-1,1-diacetate was first isolated in moderate yield (56%) and near quantitative yield of the *ortho*-hydroxy bromide (**3**) was obtained after basic hydrolysis. These two steps could be combined into a one-pot procedure. Because of the chelating potential of **3**, its hydroxyl group was converted to methoxy group by methylation with dimethyl sulfate, resulting in the formation of the *ortho*-methoxy bromide (**4**). Then, with the aid of a palladium-catalyzed amination with diphenylamine and 1,1-bis(diphenylphosphino)-ferrocene (dppf) as ligand, **AF240-OMe** (**5**) was obtained in good yield (84%). Finally, demethylation **AF240-OMe** with 2-aminothiophenol led to the isolation of **AF240-OH** (**6**) in 91% yield.

Electrochemistry

The results of cyclic voltammetry experiments are summarized in Table 1. Data were collected in acetonitrile and dichloromethane solution. Attempts to collect comparative data for **AF240-OH** in acetonitrile were unsuccessful due to limited solubility of the compound (<0.001 M). All of the complexes display reversible, one-electron oxidation waves attributed to the oxidation of the diphenylamine moiety.[45] In both solvents, **AF240** is the hardest to oxidize and **AF240-OMe** is the easiest to oxidize. This is attributed to the inductive, electron donating ability of the methoxy substituent. The anodic potentials of **AF240** and **AF240-OMe** are resilient to changes in solvent polarity as their potentials in acetonitrile are within 0.015 V of the potential values obtained in dichloromethane. The oxidation potential of **AF240-OH** falls between **AF240** and **AF240-OMe** in dichloromethane. The hydroxyl group is a weaker electron donor

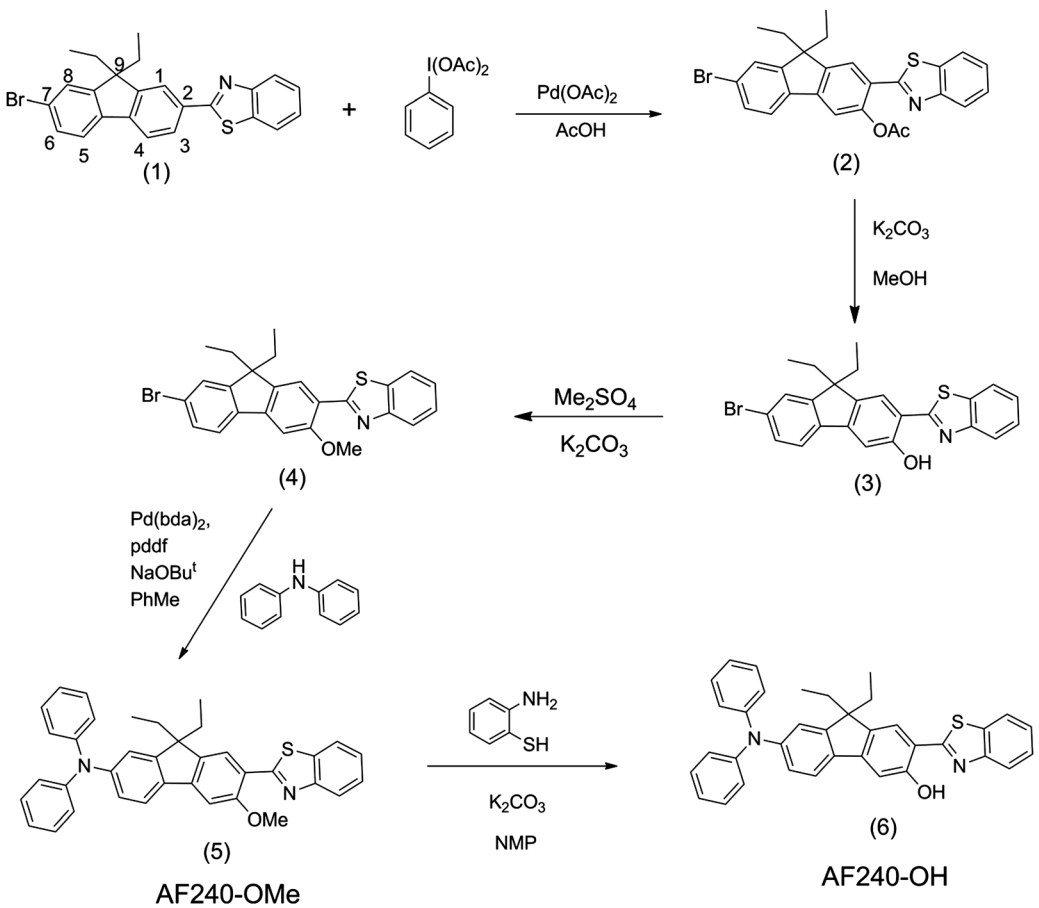

Scheme 1 Synthesis of **AF240-OMe** and **AF240-OH**.

Table 1 Redox potentials (in V) in CH_2Cl_2[a] and CH_3CN[b]

	E° (+/0)		E° (0/−)	
Compound	CH_2Cl_2	CH_3CN	CH_2Cl_2	CH_3CN
AF240	0.412	0.405	—[c]	−2.364[d]
AF240-OH	0.388	—[e]	−2.434	—[e]
AF240-OMe	0.374	0.390	—[c]	−2.412

[a] Relative to $Fc^{+/0}$ which had a potential of 0.506 V *vs.* Ag/AgCl in 4 M $KCl_{(aq)}$. [b] Relative to $Fc^{+/0}$ which had a potential of 0.496 V *vs.* Ag/AgCl in 4 M $KCl_{(aq)}$. [c] No redox couple observed within the electrochemical window of the solvent. [d] Irreversible; reported value is estimated from the peak cathodic current. [e] Unable to collect due to limited solubility in CH_3CN.

than the methoxy group. The reductive electrochemistry also provides some evidence that the hydroxyl is involved in intramolecular hydrogen bonding with the benzothiazole group (*vide infra*). The diminished donating ability of the OH group, an electronic effect from intramolecular hydrogen bonding, or some combination of the two could be the cause of the observed, anodic potential modulation in **AF240-OH**. The reductive electrochemistry is markedly different in acetonitrile and dichloromethane. In dichloromethane, no redox couple is observed within the electrochemical window of the solvent for **AF240** and **AF240-OMe**. An irreversible, cathodic wave is observed for **AF240-OH** in dichloromethane. The stabilization of the cathodic potential in **AF240-OH** in dichloromethane solution is tentatively ascribed to intramolecular hydrogen bonding between the hydroxyl group and the benzothiazole group. In acetonitrile, reversible, one-electron reduction waves are observed for both **AF240** and **AF240-OMe**. **AF240** is easier to reduce than **AF240-OMe**. This is also attributed to the inductive, donating ability of the methoxy group. The stabilization of the cathodic potential of **AF240** and **AF240-OH** in acetonitrile is attributed to electronic stabilization of the benzothiazole group in the more polar solution.

Ground-state absorption

The ground-state absorption spectra of **AF240**, **AF240-OH**, and **AF240-OMe** in five solvents of differing polarity are shown in Fig. 2. Extinction coefficients for the molecules in THF are presented in Table 2. The energy of the absorption peak maxima decreases from **AF240** > **AF240-OMe** > **AF240-OH**, regardless of solvent. Methoxy and hydroxy groups are known electron donors, suggesting the highest occupied molecular orbital (HOMO) is destabilized, resulting in the lower energy transitions observed. The hydrogen bonding ability of **AF240-OH** also lowers the lowest unoccupied molecular orbital (LUMO) energy leading to lower energy absorption transitions. These results are consistent with the electrochemical data discussed above. As observed previously,[46] the absorption spectrum of **AF240** is structured in *n*-hexane and demonstrates two resolved absorption transitions at 384 nm and 402 nm. The absorption spectrum of **AF240** evolves into a single absorption transition as solvent polarity is increased. This absorption transition arises from the coalescence of the two resolved absorption transitions.[17] This is clearly demonstrated in the observed changes in the absorption spectrum as the solvent polarity is

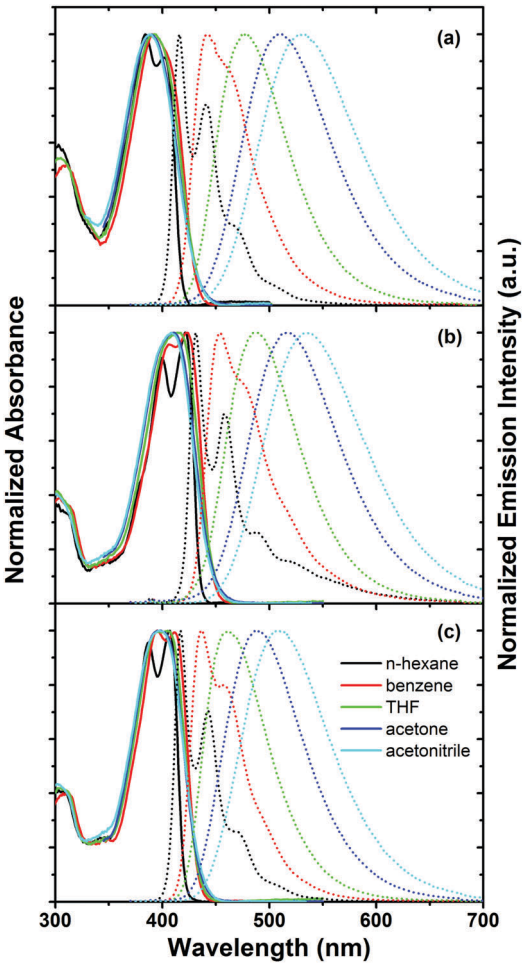

Fig. 2 Normalized absorption (solid) and emission (dotted) spectra of **AF240**-R in various solvents; R = H (a), OH (b), and OMe (c).

increased from *n*-hexane to THF. The full width at half max (FWHM) of the **AF240** absorption spectrum also increases as the solvent polarity is increased. This is attributed to enhanced ICT in the ground state of the molecule in more polar solvents. The absorption spectra of **AF240-OH** and **AF240-OMe** behave identically to the absorption spectrum of **AF240** as solvent polarity is increased. The extinction coefficients in THF for methoxy and hydroxy derivatives are slightly higher than **AF240**, as the electronic effects induced by the substituents likely increase the oscillator strength.

Luminescence

The steady-state emission spectra (Fig. 2 and Table 2) show significant solvatochromism for all chromophores, as the emission spectra undergo a bathochromic shift and broaden as the solvent polarity increases. This is consistent with transition from a locally excited (LE) state in nonpolar solvents to an ICT state in polar solvents, as described previously.[46,47] The different solvent regimes (nonpolar *vs.* polar) affect the excited state energies of the chromophores differently. In nonpolar solvents, the emission energies of the **AF240** and **AF240-OMe** derivatives are nearly isoenergetic, while emission from **AF240-OH**

Table 2 Absorption and emission properties of the dyes in various solvents

	Solvent	λ_{abs}/nm	ε/M^{-1} cm^{-1} [a]	λ_{em}/nm	Stokes shift/eV	Φ_{fl}	τ/ns	$k_r/10^8$ s^{-1}	$k_{nr}/10^8$ s^{-1}
AF240	*n*-Hexane	402		416	0.10	0.79	1.20	6.59	1.76
	Benzene	393		442	0.35	0.88	1.49	5.90	0.80
	THF	393	44 400	477	0.56	0.92	2.04	4.50	0.41
	Acetone	390		509	0.74	0.89	2.59	3.44	0.43
	Acetonitrile	388		531	0.86	0.84	2.98	2.81	0.54
AF240-OH	*n*-Hexane	422		431	0.06	0.39	0.83	4.67	7.32
	Benzene	423		454	0.20	0.56	1.03	5.37	4.30
	THF	415	49 500	487	0.44	0.72	1.56	4.66	1.77
	Acetone	411		516	0.61	0.73	2.30	3.17	1.18
	Acetonitrile	408		535	0.72	0.68	2.77	2.44	1.17
AF240-OMe	*n*-Hexane	407		417	0.07	1	1.20	8.35	<0.1
	Benzene	411		436	0.17	1	1.37	7.31	<0.1
	THF	405	49 300	461	0.37	0.92	1.74	5.26	0.490
	Acetone	399		488	0.57	0.91	2.17	4.19	0.43
	Acetonitrile	398		510	0.68	0.90	2.56	3.50	0.410

[a] Extinction coefficients were only measured in THF solution.

occurs at lower energy. As the solvent polarity increases, **AF240-OMe** becomes the highest energy emitter followed by **AF240** then **AF240-OH**. The emission energy of **AF240** is nearly identical to the energy of **AF240-OH** in acetonitrile. The hydroxy and methoxy substituents can influence the emission energies in three ways: (1) *via* electronic affects, (2) *via* steric affects and (3) *via* induced hydrogen bonding to the benzothiazole group in the case of the hydroxy derivative. When first examining the data in nonpolar solvents, it is notable that the emission energies of **AF240** and **AF240-OMe** are nearly isoenergetic, despite the fact that the **AF240-OMe** has lower energy ground state absorption. This is likely caused by the steric bulk of the methoxy group preventing planarization of the benzothiazole with the fluorene in the excited state, which is known to be favored from previous calculations.[28] The inability to planarize decreases the extent of ICT, leading to less LUMO stabilization and higher emission energies. This trend of increased emission energies in **AF240-OMe** is observed for all solvent polarities. In the case of the **AF240-OH**, hydrogen bonding between the hydroxy group and the nonpolar solvent is unfavorable. This leads to forced hydrogen bonding with the benzothiazole group (Fig. 3), which has been observed in HBT.[29] This lowers the LUMO energy and leads to the red shift observed in both the absorption and emission maxima in nonpolar solvents. In polar solvents, hydrogen bonding to the solvent (THF, acetone, or acetonitrile) can occur. This limits the stabilization of the LUMO *via* hydrogen bonding to the benzothiazole.

As observed previously for **AF240**, the lifetimes increase with increasing solvent polarity.[46] This has been attributed to a state change from LE to ICT, with the radiative rate constant, k_r, decreasing as the excited-state character becomes more ICT-like. A plot of the inverse lifetime as a function of the maximum emission energy (Fig. 4) shows that the rate of excited state deactivation increases as the emission energy increases. **AF240** and **AF240-OMe** follow a nearly identical linear decrease in lifetime with increasing solvent polarity. However, **AF240-OH** deviates from this trend as the lifetimes are significantly shorter in the nonpolar solvents. This is attributed to increased

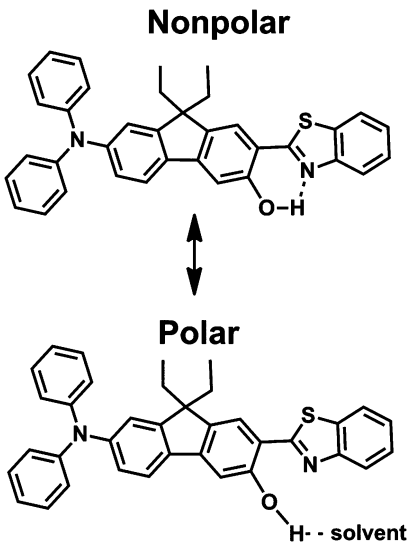

Fig. 3 Hydrogen bonding scheme of **AF240-OH** in nonpolar (top) and polar (bottom) solvents.

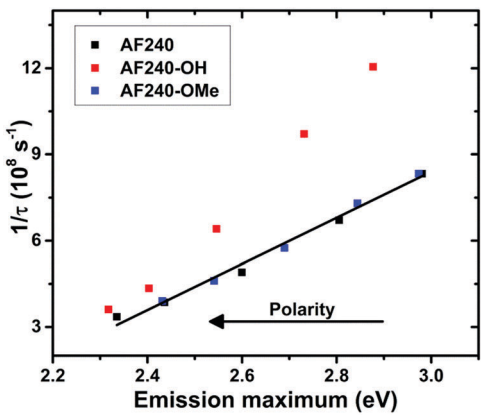

Fig. 4 Excited-state decay rate constant as a function of emission maxima.

vibrational decay pathways induced *via* intramolecular hydrogen bonding between the hydroxy group and the benzothiazole in nonpolar solvents, supporting the conclusions above, and consistent with previous work.[29,36,37] The lifetimes begin to converge toward the line formed by **AF240**/**AF240-OMe** as the emission energy decreases, although they are still slightly shorter. This supports a change from intramolecular hydrogen bonding to intermolecular hydrogen bonding with increasing hydrogen bonding ability of the solvent. The hydrogen bonding impact on the nonradiative rate constant, k_{nr}, is much greater in the intramolecular case, but there still appears to be an attributable k_{nr} increase when hydrogen bonding occurs intermolecularly with the polar solvents.

In the cases of **AF240** and **AF240-OMe**, the fluorescence quantum yields, Φ_{fl} (Table 2) are relatively independent of solvent polarity, with those of the methoxy derivative being slightly larger than **AF240**. It should be noted that the values reported here are different than previously reported for **AF240**[28,46] due to the acquisition of an integrating sphere which provides more reliable, absolute quantum yield values. Calculations of k_r and k_{nr} from the quantum yields and lifetimes for **AF240** and **AF240-OMe** show that k_r decreases as the solvent polarity increases and the excited state changes from LE to ICT in nature. The luminescence behavior of **AF240-OH** is markedly different. The luminescence quantum yield increases as the solvent polarity increases. The lower quantum yield values in nonpolar solvents are driven by an increase in k_{nr}, consistent with increased vibrational decay induced by intramolecular hydrogen bonding. The quantum yields in the polar solvents for **AF240-OH** are lower than that of the other two molecules; coupled with larger values of k_{nr}, this shows some deactivation is also likely *via* hydrogen bonding to the solvent.

Transient absorption

The femtosecond transient absorption spectra of **AF240**, **AF240-OH**, and **AF240-OMe** in THF solution at varying time delays are shown in Fig. 5. The **AF240** results have been previously discussed in detail.[46] Briefly, some ICT has already occurred within the instrument response of the experiment. Further stabilization of this state is observed as the peak maximum at 620 nm undergoes a hypsochromic shift over the first few ps due to a combination of solvent and geometric relaxations to yield a solvent-stabilized intramolecular charge-transfer (SSICT) state. Very similar effects are observed for both **AF240-OH** and **AF240-OMe** as hypsochromic shifts of the peak maxima are observed over the first few ps after excitation. The most remarkable changes are in the magnitude of the shifts in the peak maxima from time zero to 10 ps (Table 3). **AF240** and **AF240-OH** shift 21 and 19 nm, respectively, but **AF240-OMe** shifts only eight nm. This difference could be explained by less stabilization of the SSICT state relative to the ICT state and supports the hypothesis that the bulkier methoxy group inhibits geometric relaxation of the excited state.

Three lifetimes are observed for each molecule. The first component is around two ps for all three and corresponds to solvent and geometric reorganization. The second lifetime ranges from 78 to 223 ps, but it is unclear as to what this corresponds. No spectral changes are observed over this time range, so there is currently no explanation as to its origin. The third lifetime closely matches the lifetime obtained from time-resolved fluorescence and corresponds to the decay of the excited state.

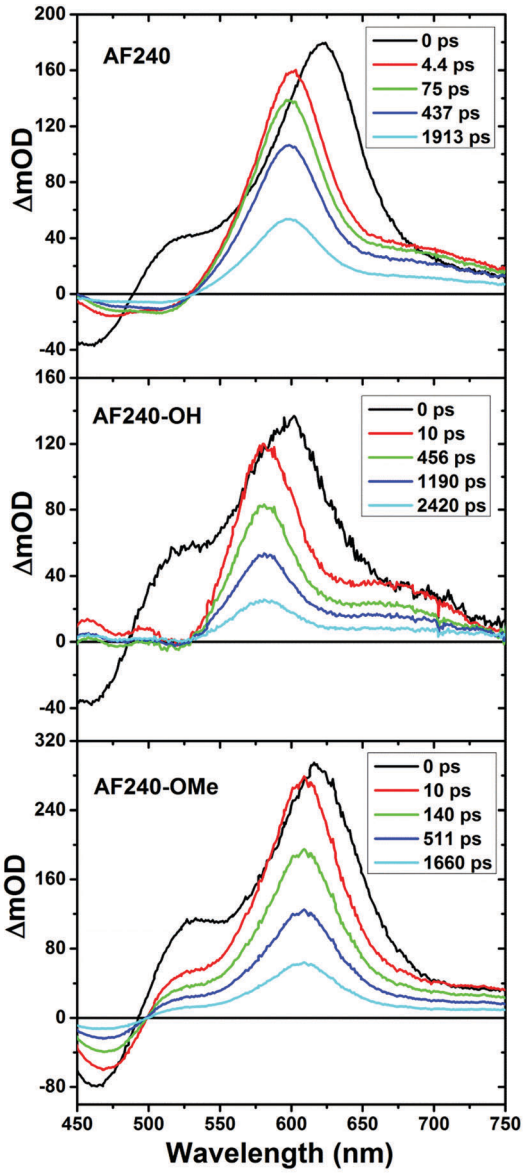

Fig. 5 Transient absorption difference spectra of **AF240**, **AF240-OH**, and **AF240-OMe** in THF solution following 400 nm excitation.

Table 3 Femtosecond transient absorption properties in tetrahydrofuran solution[a]

Compound	λ_{max}/nm t = 0 ps	λ_{max}/nm t = 10 ps	τ_1/ps	τ_2/ps	τ_3/ps
AF240	622	601	2.38(2.12)	77.8(38.0)	1940(110)
AF240-OH	600	581	1.75(0.44)	223(24)	1670(30)
AF240-OMe	616	608	2.55(0.95)	119(4)	1750(130)

[a] Error shown in parentheses.

Two photon absorption

To discern the influence of coplanarity driven by intramolecular hydrogen bonding in this D–π–A system on two-photon absorption, 2PA spectral measurements of **AF240** and **AF240-OH** in THF solutions were conducted by a femtosecond two-photon-induced fluorescence (2PIF) method.[41] The superimposed 1PA and 2PA spectra of **AF240** and **AF240-OH** are depicted in Fig. 6a and b for easy comparison. As shown in Fig. 6a, the parent **AF240** molecule has a peak at λ_{max}(2PA) = 810 nm, corresponding to an intrinsic 2PA cross-section (σ_2) value of ~560 GM. Unlike **AF240** whose 2PA spectrum is slightly red-shifted from the theoretical excitation wavelength (780 nm), both the peak regions of 1P and 2P spectra of **AF240-OH** (Fig. 6b) are quite congruent in the NIR region (~750–900 nm) and visible region (550–650 nm). In addition, a new 2PA band in the visible region (650–750 nm) for **AF240-OH**, having the λ_{max}(2PA) at ~705 nm with σ_2 ~ 600 GM, which is slightly higher than the σ_2 associated with the 2PA band (810 nm; NIR) with σ_2 ~ 500 GM. In conjunction with a similar 2PA spectrum that has been reported for a related (2-hydroxyphenyl-benzothiazole)-vinylfluorene chromophore,[48] the deviation from the typically observed 2PA spectra of dipolar AFX chromophores as exemplified by **AF240** implicates a more complex set of excited state structures may be involved in the nonlinear absorption process of **AF240-OH**. Based on the possibility of a coupled process of ESIPT and solvent stabilized ICT, it is proposed (Scheme 2) that the 2PA band upon fs NIR excitation is associated with the solvent stabilized (SS) and planar **AF240-OH** (SS-PICT) and the band upon fs visible excitation is associated with the twisted, keto-tautomer (SS-TICT). With the higher negative charge density localized on one of the phenyl rings of the fluorene structure and the electron-deficient quinoidal moiety formed in the other phenyl ring, this excited state TICT structure is formally a D–π–A with conjugation length shorter than that in the PICT structure. Our tentative assignment of 2PA band in the visible region (TICT) is supported by a report that 2-(2-hydroxyphenyl)-benzothiazole (HBT) itself was 2PA-responsive in the visible region upon picosecond laser irradiation at 532 nm,[49] and based on the fact that the ICT character and conjugation length of TICT should be greater than those in HBT molecule. While the maximal value of intrinsic 2PA cross-section of **AF240-OH** is moderately (20%) higher than that of **AF240**, it is apparent that the intramolecular hydrogen bonding in **AF240-OH** has greatly expanded the wavelength range for 2PA sensitivity, for example, at a minimum of 200 GM, ~630–880 nm ($\Delta\lambda$ ~ 250 nm) for **AF240-OH** *vs.* ~770–860 nm ($\Delta\lambda$ ~ 90 nm) for **AF240** (Fig. 6a and b).

On the other hand, when the longer-range ICT process, *i.e.* from diphenylamine to benzothiazole, in **AF240-OMe** in excited state is severely disrupted by having the methoxy substituent forcing the benzothiazole unit to be out of plane with the rest of the conjugated system, and the adverse effect accentuated by the inductive (+I) effect of methoxy on the π-excess benzothiazole moiety, much smaller 2PA cross-sections[42] are observed: 45 GM (675 nm) and 25 GM (820 nm) (Fig. 6c). The two well-defined 2PA bands are postulated to be originated from the shorter-range ICT involving methoxy-benzothiazole (675 nm) and the longer-range-diphenylamine-benzothiazole (820 nm).

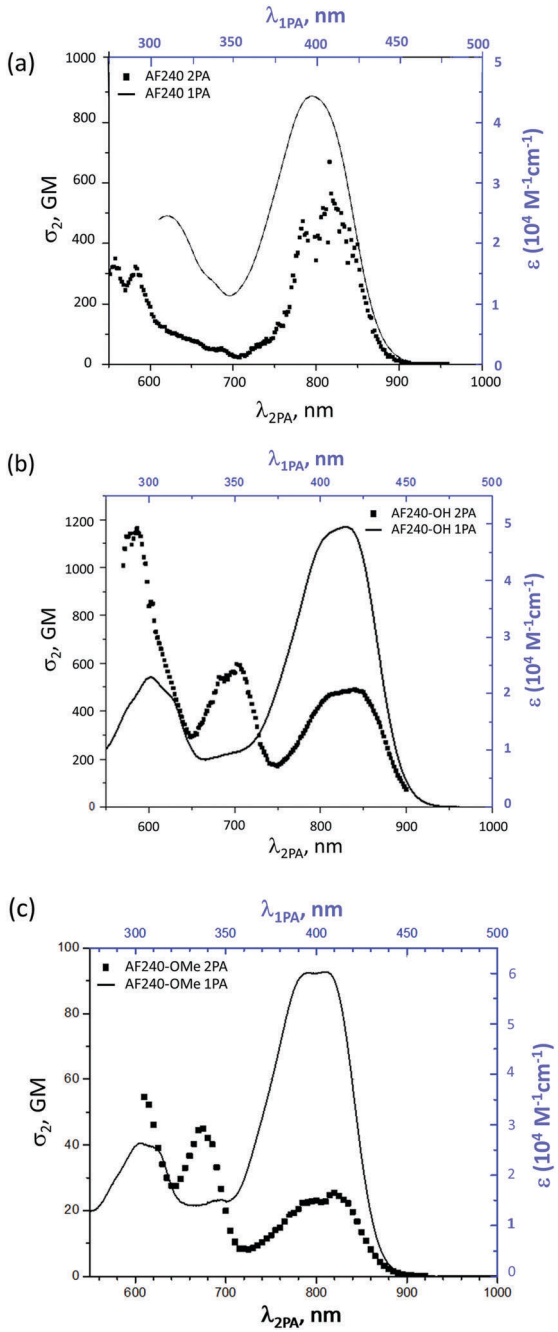

Fig. 6 Superimposed 1PA (solid curve) & 2PA (filled squares) spectra of (a) **AF240** and (b) **AF240-OH**; (c) **AF240-OMe** taken in THF.

Conclusions

Both new derivatives (**AF240-OH** and **AF240-OMe**) show general trends consistent with **AF240:** (i) broadening of the ground-state absorption and luminescence spectra with increasing solvent polarity; (ii) significant solvatochromism in the emission energies; and (iii) a hypsochromic shift in the peak maxima observed by

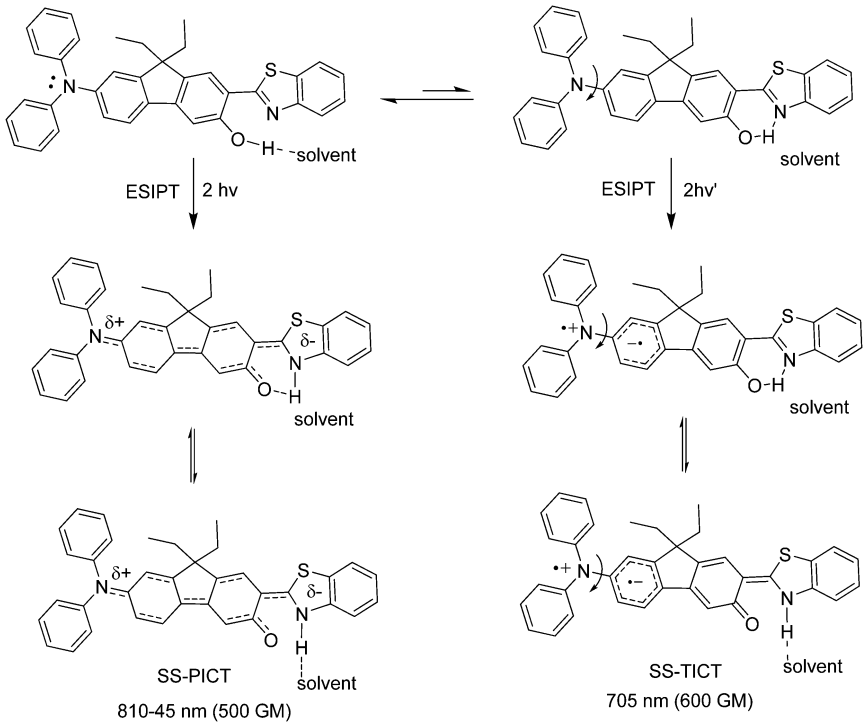

Scheme 2 Proposed excited species in solvent-stabilized ICT processes (SS-TICT and SS-PICT) that are involved in the fs 2PA process of **AF240-OH**. The excited state ESIPT equilibria of both SS-ICT is fast so that the tautomeric structure is likely to be the intermediate between the NH···N and OH···N forms when not hydrogen-bonded with polar solvent molecule.

ultrafast transient absorption. These results are consistent with a state change from LE in nonpolar solvents to ICT in polar solvents, with geometric and solvent reorganizations ultimately leading to a SSICT state. The observed differences in the molecules caused by the addition of the hydroxy and methoxy groups lie in the energetics and excited state dynamics. Electrochemical data support destabilization of the HOMO in **AF240-OH** and **AF240-OMe** due to inductive electron-donating ability. The LUMO is stabilized in **AF240-OH** *via* intramolecular hydrogen bonding, but is destabilized in **AF240-OMe**, again due to the electron-donating ability. The ground-state results are generally consistent with these data, with the energies trending from **AF240** > **AF240-OMe** > **AF240-OH**. The fluorescence data support intramolecular hydrogen bonding in **AF240-OH** in nonpolar solvents, which switches to intermolecular hydrogen bonding to solvent with increasing polarity. The nonradiative decay rate constants increase due to additional vibrational decay pathways created by the hydrogen bonding. The increase in k_{nr} is larger in the case of the intramolecular hydrogen bonding in nonpolar solvents. As ICT character increases with increasing solvent polarity, it is known that the fluorene and benzothiazole moieties want to planarize. The increased emission energies in **AF240-OMe** as well as smaller hypsochromic shifts observed in the femtosecond TA data suggest that the methoxy group hinders planarization. While the results are not overly dramatic, they do show that modulation of the excited-state energies and lifetimes occurs *via* intramolecular hydrogen bonding. The decrease in emission energies in the case of **AF240-OH** support increased ICT driven by higher degree of coplanarity and the quinoidal structure in the excited state. However, a moderate increase in the intrinsic 2PA cross-section is observed. It is likely because of the two possible and competing ICT processes (PICT and TICT) in **AF240-OH**. Nevertheless, the strategic presence of an OH group capable of intramolecular hydrogen bonding in **AF240-OH** provides a much broader 2PA sensitivity window than **AF240**.

Conflicts of interest

There are no conflicts to declare.

Acknowledgements

Funding support was provided by AFRL/AFOSR and AFRL/RX Directorates, Air Force Research Laboratory. We are grateful to Dr Aleks Rebane (Montana State University) for the femtosecond 2PA spectral measurements.

References

1 F. Helmchen and W. Denk, *Nat. Methods*, 2005, **2**, 932–940.
2 W. R. Zipfel, R. M. Williams and W. W. Webb, *Nat. Biotechnol.*, 2003, **21**, 1369–1377.
3 W. Min, C. W. Freudiger, S. Lu and X. S. Xie, *Annu. Rev. Phys. Chem.*, 2011, **62**, 507–530.

4 C. N. LaFratta, J. T. Fourkas, T. Baldacchini and R. A. Farrer, *Angew. Chem., Int. Ed. Engl.*, 2007, **46**, 6238–6258.
5 K.-S. Lee, D.-Y. Yang, S. H. Park and R. H. Kim, *Polym. Adv. Technol.*, 2006, **17**, 72–82.
6 W. G. Fisher, W. P. Partridge, Jr., C. Dees and E. A. Wachter, *Photochem. Photobiol.*, 1997, **66**, 141–155.
7 C. W. Spangler, *J. Mater. Chem.*, 1999, **9**, 2013–2020.
8 S.-J. Chung, K.-S. Kim, T.-C. Lin, G. S. He, J. Swiatkiewicz and P. N. Prasad, *J. Phys. Chem. B*, 1999, **103**, 10741–10745.
9 S. R. Marder, *Chem. Commun.*, 2006, 131–134, DOI: 10.1039/B512646K.
10 C. Katan, F. Terenziani, O. Mongin, M. H. Werts, L. Porres, T. Pons, J. Mertz, S. Tretiak and M. Blanchard-Desce, *J. Phys. Chem. A*, 2005, **109**, 3024–3037.
11 A. Bhaskar, G. Ramakrishna, Z. Lu, R. Twieg, J. M. Hales, D. J. Hagan, E. Van Stryland and T. Goodson, 3rd, *J. Am. Chem. Soc.*, 2006, **128**, 11840–11849.
12 A. Qin, C. K. W. Jim, W. Lu, J. W. Y. Lam, M. Häussler, Y. Dong, H. H. Y. Sung, I. D. Williams, G. K. L. Wong and B. Z. Tang, *Macromolecules*, 2007, **40**, 2308–2317.
13 K. S. Kim, S. B. Noh, T. Katsuda, S. Ito, A. Osuka and D. Kim, *Chem. Commun.*, 2007, 2479–2481, DOI: 10.1039/b704986b.
14 M. Fakis, I. Fitilis, S. Stefanatos, P. Vellis, J. Mikroyannidis, V. Giannetas and P. Persephonis, *Dyes Pigm.*, 2009, **81**, 63–68.
15 J.-Z. Cheng, C.-C. Lin, P.-T. Chou, A. Chaskar and K.-T. Wong, *Tetrahedron*, 2011, **67**, 734–739.
16 G. Ramakrishna and T. Goodson, 3rd, *J. Phys. Chem. A*, 2007, **111**, 993–1000.
17 K. A. Nguyen, J. E. Rogers, J. E. Slagle, P. N. Day, R. Kannan, L. S. Tan, P. A. Fleitz and R. Pachter, *J. Phys. Chem. A*, 2006, **110**, 13172–13182.
18 O. Mongin, L. Porrès, M. Charlot, C. Katan and M. Blanchard-Desce, *Chem. – Eur. J.*, 2007, **13**, 1481–1498.
19 W. J. Yang, D. Y. Kim, M. Y. Jeong, H. M. Kim, Y. K. Lee, X. Fang, S. J. Jeon and B. R. Cho, *Chem. – Eur. J.*, 2005, **11**, 4191–4198.
20 B. A. Reinhardt, L. L. Brott, S. J. Clarson, A. G. Dillard, J. C. Bhatt, R. Kannan, L. Yuan, G. S. He and P. N. Prasad, *Chem. Mater.*, 1998, **10**, 1863–1874.
21 R. Kannan, G. S. He, L. Yuan, F. Xu, P. N. Prasad, A. G. Dombroskie, B. A. Reinhardt, J. W. Baur, R. A. Vaia and L.-S. Tan, *Chem. Mater.*, 2001, **13**, 1896–1904.
22 K. D. Belfield, D. J. Hagan, E. W. Van Stryland, K. J. Schafer and R. A. Negres, *Org. Lett.*, 1999, **1**, 1575–1578.
23 R. Kannan, G. S. He, T.-C. Lin, P. N. Prasad, R. A. Vaia and L.-S. Tan, *Chem. Mater.*, 2004, **16**, 185–194.
24 K. D. Belfield, A. R. Morales, B.-S. Kang, J. M. Hales, D. J. Hagan, E. W. Van Stryland, V. M. Chapela and J. Percino, *Chem. Mater.*, 2004, **16**, 4634–4641.
25 W. V. Moreshead, O. V. Przhonska, M. V. Bondar, A. D. Kachkovski, I. H. Nayyar, A. E. Masunov, A. W. Woodward and K. D. Belfield, *J. Phys. Chem. C*, 2013, **117**, 23133–23147.
26 T.-H. Huang, D. Yang, Z.-H. Kang, E.-L. Miao, R. Lu, H.-P. Zhou, F. Wang, G.-W. Wang, P.-F. Cheng, Y.-H. Wang and H.-Z. Zhang, *Opt. Mater.*, 2013, **35**, 467–471.
27 J. E. Rogers, J. E. Slagle, D. G. McLean, R. L. Sutherland, M. C. Brant, J. Heinrichs, R. Jakubiak, R. Kannan, L. S. Tan and P. A. Fleitz, *J. Phys. Chem. A*, 2007, **111**, 1899–1906.
28 D. J. Stewart, M. J. Dalton, S. L. Long, R. Kannan, Z. Yu, T. M. Cooper, J. E. Haley and L. S. Tan, *Phys. Chem. Chem. Phys.*, 2016, **18**, 5587–5596.
29 S. M. Aly, A. Usman, M. AlZayer, G. A. Hamdi, E. Alarousu and O. F. Mohammed, *J. Phys. Chem. B*, 2015, **119**, 2596–2603.
30 S. Luber, K. Adamczyk, E. T. J. Nibbering and V. S. Batista, *J. Phys. Chem. A*, 2013, **117**, 5269–5279.
31 T. Iijima, A. Momotake, Y. Shinohara, T. Sato, Y. Nishimura and T. Arai, *J. Phys. Chem. A*, 2010, **114**, 1603–1609.
32 S. Lochbrunner, A. J. Wurzer and E. Riedle, *J. Chem. Phys.*, 2000, **112**, 10699–10702.
33 S. R. Vazquez, M. C. R. Rodriguez, M. Mosquera and F. Rodriguez-Prieto, *J. Phys. Chem. A*, 2007, **111**, 1814–1826.
34 H.-W. Tseng, J.-Q. Liu, Y.-A. Chen, C.-M. Chao, K.-M. Liu, C.-L. Chen, T.-C. Lin, C.-H. Hung, Y.-L. Chou, T.-C. Lin, T.-L. Wang and P.-T. Chou, *J. Phys. Chem. Lett.*, 2015, **6**, 1477–1486.
35 H. Shimada, A. Nakamura, T. Yoshihara and S. Tobita, *Photochem. Photobiol. Sci.*, 2005, **4**, 367–375.
36 I. Petkova, G. Dobrikov, N. Banerji, G. Duvanel, R. Perez, V. Dimitrov, P. Nikolov and E. Vauthey, *J. Phys. Chem. A*, 2010, **114**, 10–20.
37 S. Lin and W. S. Struve, *Photochem. Photobiol.*, 1991, **54**, 361–365.
38 V. S. Padalkar, D. Sakamaki, K. Kuwada, A. Horio, H. Okamoto, N. Tohnai, T. Akutagawa, K.-i. Sakai and S. Seki, *Asian J. Org. Chem.*, 2016, **5**, 938–945.
39 D. B. G. Williams and M. Lawton, *J. Org. Chem.*, 2010, **75**, 8351–8354.
40 A. V. Nikolaitchik, O. Korth and M. A. J. Rodgers, *J. Phys. Chem. A*, 1999, **103**, 7587–7596.
41 N. S. Makarov, M. Drobizhev and A. Rebane, *Opt. Express*, 2008, **16**, 4029–4047.
42 S. de Reguardati, J. Pahapill, A. Mikhailov, Y. Stepanenko and A. Rebane, *Opt. Express*, 2016, **24**, 9053–9066.
43 A. Aydin, H. Soylu, M. Akkurt, C. Arici and M. Erdemir, *Z. Kristallogr. – New Cryst. Struct.*, 1999, **214**, 529–530.
44 A. Banerjee, A. Bera, S. Guin, S. K. Rout and B. K. Patel, *Tetrahedron*, 2013, **69**, 2175–2183.
45 E. T. Seo, R. F. Nelson, J. M. Fritsch, L. S. Marcoux, D. W. Leedy and R. N. Adams, *J. Am. Chem. Soc.*, 1966, **88**, 3498–3503.
46 D. J. Stewart, M. J. Dalton, R. N. Swiger, J. L. Fore, M. A. Walker, T. M. Cooper, J. E. Haley and L. S. Tan, *J. Phys. Chem. A*, 2014, **118**, 5228–5237.
47 J. E. Rogers, J. E. Slagle, D. G. McLean, R. L. Sutherland, B. Sankaran, R. Kannan, L.-S. Tan and P. A. Fleitz, *J. Phys. Chem. A*, 2004, **108**, 5514–5520.
48 A. R. Morales, K. J. Schafer-Hales, C. O. Yanez, M. V. Bondar, O. V. Przhonska, A. I. Marcus and K. D. Belfield, *ChemPhysChem*, 2009, **10**, 2073–2081.
49 J. Zheng, Y. Guo, X. Li, G. Zhang and W. Chen, *J. Opt. A: Pure Appl. Opt.*, 2006, **8**, 835–839.